AJNR

In Vitro and In Vivo Imaging Characteristics Assessment of Polymeric Coils Compared with Standard Platinum Coils for the Treatment of Intracranial Aneurysms

P. Mordasini, A.K. Kraehenbuehl, J.V. Byrne, S. Vandenberghe, M. Reinert, H. Hoppe and J. Gralla

This information is current as of June 3, 2025.

AJNR Am J Neuroradiol 2013, 34 (11) 2177-2183
doi: https://doi.org/10.3174/ajnr.A3589
http://www.ajnr.org/content/34/11/2177

In Vitro and In Vivo Imaging Characteristics Assessment of Polymeric Coils Compared with Standard Platinum Coils for the Treatment of Intracranial Aneurysms

P. Mordasini, A.K. Kraehenbuehl, J.V. Byrne, S. Vandenberghe, M. Reinert, H. Hoppe, and J. Gralla

ABSTRACT

BACKGROUND AND PURPOSE: Conventional platinum coils cause imaging artifacts that reduce imaging quality and therefore impair imaging interpretation on intraprocedural or noninvasive follow-up imaging. The purpose of this study was to evaluate imaging characteristics and artifact production of polymeric coils compared with standard platinum coils in vitro and in vivo.

MATERIALS AND METHODS: Polymeric coils and standard platinum coils were evaluated in vitro with the use of 2 identical silicon aneurysm models coiled with a packing attenuation of 20% each. DSA, flat panel CT, CT, and MR imaging were performed. In vivo evaluation of imaging characteristics of polymeric coils was performed in experimentally created rabbit carotid bifurcation aneurysms. DSA, CT/CTA, and MR imaging were performed after endovascular treatment of the aneurysms. Images were evaluated regarding visibility of individual coils, coil mass, artifact production, and visibility of residual flow within the aneurysm.

RESULTS: Overall, in vitro and in vivo imaging showed relevantly reduced artifact production of polymeric coils in all imaging modalities compared with standard platinum coils. Image quality of CT and MR imaging was improved with the use of polymeric coils, which permitted enhanced depiction of individual coil loops and residual aneurysm lumen as well as the peri-aneurysmal area. Remarkably, CT images demonstrated considerably improved image quality with only minor artifacts compared with standard coils. On DSA, polymeric coils showed transparency and allowed visualization of superimposed vessel structures.

CONCLUSIONS: This initial experimental study showed improved imaging quality with the use of polymeric coils compared with standard platinum coils in all imaging modalities. This might be advantageous for improved intraprocedural imaging for the detection of complications and posttreatment noninvasive follow-up imaging.

ABBREVIATION: FP-CT = flat panel CT

After the International Subarachnoid Aneurysm Trial (ISAT) study,[1] endovascular treatment of cerebral aneurysms with the use of platinum coils has become the main treatment technique for cerebral aneurysms in most of the centers worldwide. However, approximately 20% of coiled aneurysms demonstrate signs of recanalization in their further course,[2-5] which is more likely to occur in large or giant and wide-neck aneurysms.[6,7] As a result, routine posttreatment imaging follow-up for coiled aneurysms is mandatory to detect re-growth and to determine the need for re-treatment.

However, current coil systems are made of platinum alloy, which is prone to artifact production during imaging. Imaging artifacts induced by platinum coils may significantly reduce imaging quality and influence interpretation of noninvasive follow-up imaging with the use of MRI/MRA preventing adequate diagnosis of residual intra-aneurysmal flow and areas close to the treated aneurysm. Furthermore, extensive metal-induced beam-hardening and streak artifacts deteriorate imaging quality and significantly impair the diagnostic accuracy of postprocedural CT scans, important for the recognition and management of complications, such as re-bleedings and aneurysm rupture during endovascular treatment. Moreover, even during endovascular treatment procedures, coil artifacts may impair the ability to optimally

Received November 14, 2012; accepted after revision February 23, 2013.

From the Institute of Diagnostic and Interventional Neuroradiology (P.M., J.G.) and Institute of Diagnostic, Pediatric, and Interventional Radiology (H.H.), Inselspital; Department of Neurosurgery (A.K.K., M.R.); and ARTORG Center for Biomedical Engineering Research (S.V.), University of Bern, Bern, Switzerland; and Neurovascular and Neuroradiology Research Unit (J.V.B.), Nuffield Department of Surgery, The John Radcliffe Hospital, University of Oxford, Oxford, United Kingdom.

P.M. was supported by a scientific grant from the Swiss Foundation for Grants in Biology and Medicine (SFGBM).

Please address correspondence to Pasquale Mordasini, MD, MSc, Department of Diagnostic and Interventional Neuroradiology, Inselspital, University of Bern, Freiburgstr 4, CH-3010 Bern, Switzerland; e-mail: pasquale.mordasini@insel.ch

Indicates open access to non-subscribers at www.ajnr.org

Indicates article with supplemental on-line table

http://dx.doi.org/10.3174/ajnr.A3589

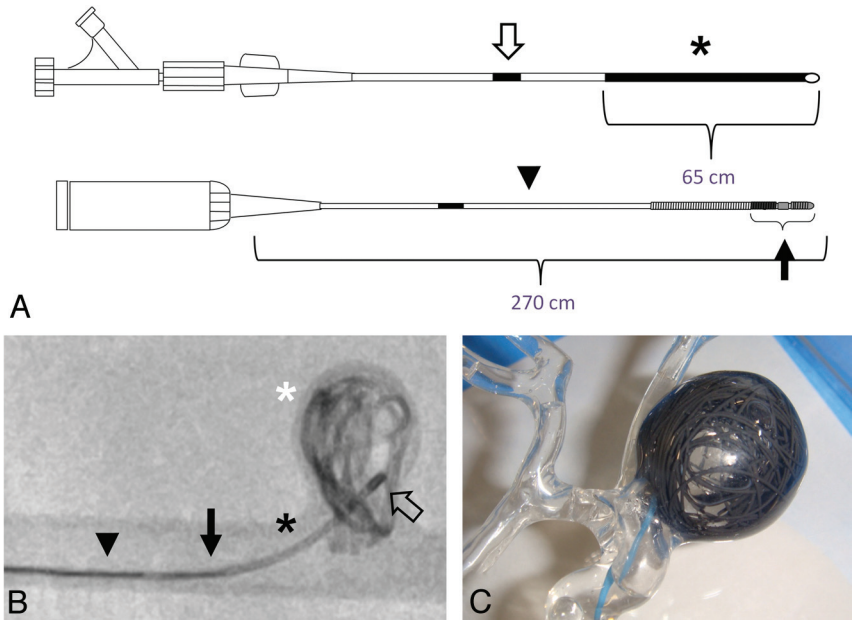

FIG 1. *A,* Schematic illustration of the polymeric coil system (above) and the delivery/detacher device (below). The coil system consists of a proximal shaft (*open arrow,* ink marker) attached to a hemostatic valve and a distal 65-cm-long radiopaque polymeric strand with an outer diameter of 0.018 inch (*asterisk*). The delivery/detacher device (total length, 270 cm) is introduced through the hemostatic valve into the inner lumen of the coil system. The delivery/detacher device consists of the microwire (*arrowhead*) and the heater coil attached to its distal tip (*arrow*). *B,* Fluoroscopy of an in vitro silicon aneurysm model showing the radiopaque polymeric strand (*black asterisk*) within the microcatheter placed in the aneurysm (microcatheter tip, *open arrow*) and its unfolded distal part within the aneurysm sac (*white asterisk*). Note the radiopaque section of the heater coil (*arrow*) at the distal tip of the delivery/detacher device (*arrowhead*) running within the coil strand. The polymeric strand can be detached at any point by advancing the radiopaque section of the heater coil at the level of the microcatheter tip and activating the thermal detachment. *C,* Photographic depiction of the silicon aneurysm model after introduction of the polymeric coil.

visualize the vessel anatomy on DSA by superimposing vessel structures of interest, such as branches arising from or close to the aneurysmal neck, especially in larger aneurysms and aneurysms with a complex anatomy.[8-16]

Therefore, from an imaging point of view, the optimal coil material should be the least prone to imaging artifacts as possible to permit optimal visualization of the vessel anatomy and adjacent brain tissue for endovascular treatment as well as for follow-up imaging. Metal-free, polymeric material potentially offers the ability for reduced artifact production compared with platinum. To date, only limited data about polymeric-based embolization material for endovascular treatment of cerebral aneurysms are available in the literature.[17-19]

The purpose of this study was to evaluate the imaging characteristics and artifact production of a polymeric coil system for the treatment of intracranial aneurysms compared with standard platinum coils.

MATERIALS AND METHODS

We compared the imaging characteristics of standard platinum coils and polymeric coils in vitro with the use of a silicon model, with DSA, flat panel CT (FP-CT), CT, and MR imaging. Furthermore, imaging characteristics of polymeric coils were assessed in vivo with the use of an experimental rabbit carotid bifurcation aneurysm model, with DSA, CT, CTA, and MR imaging.

Embolic Devices: Polymeric Coil System and Standard GDC-18 Coils

The detachable polymeric coil system (cPAX; NeuroVasx, Maple Grove, Minnesota) was approved in 2011 by the US Food and Drug Administration for the treatment of large intracranial aneurysms. The coil system consists of a proximal shaft and a distal section of detachable polymeric strand (65 cm long, 0.018-inch outer diameter) with an inner lumen to introduce the delivery/detacher device. The polymeric strand has tantalum incorporated within to gain radio-opacity to assist during navigation and placement under fluoroscopy. The shaft has an ink mark to indicate when fluoroscopic guidance is required. A manifold with a rotating hemostatic valve is attached at the proximal end for flushing the coil system before use and to introduce the delivery/detacher device. The delivery/detacher device is a 0.011-inch microwire device consisting of a core with an electric lead wire attached to a heater coil at its distal end. It is intended for the delivery of the polymer strand into the aneurysm and subsequent thermal detachment. The distal end of the device is radiopaque to assist in guidance and placement of the device under fluoroscopy. The delivery/detacher device is packaged within the lumen of the coil system and can be moved within the inner lumen to assist navigation of the strand for deployment within the aneurysm. The proximal end of the delivery/detacher device consists of an electrical connector, which is connected via a jumper cable to a power supply box for detachment. The polymeric strand and the delivery/detacher device within it are delivered into a cerebral aneurysm through a standard 0.021F microcatheter by use of the same delivery technique as the currently used platinum coil technology. The strand is fully retrievable before detachment. Thermal detachment can be accomplished at any point along the polymer strand by placing the heater coil under fluoroscopic control at the tip of the microcatheter. The strand design of the device and the thermal detachment by use of the heater coil within the strand allow continuous filling of the aneurysms and detachment at any point versus the fixed detachment zone of a standard platinum coil (Fig 1).

To compare imaging characteristics with standard platinum coils in vitro with a comparable diameter, GDC-18 coils (0.018-inch outer diameter; Boston Scientific/Stryker Neurovascular, Natick, Massachusetts) were used for embolization of an identical silicon model in standard coiling technique.

In Vitro Experimental Setup

Two identical commercially available silicon models of a large wide-neck right internal carotid artery aneurysm (diameter, 23 mm; neck, 5.7 × 8.2 mm; Elastrat, Geneva, Switzerland) were

used for coiling with polymeric coils and standard platinum coils. Both aneurysms were coiled up to a calculated packing attenuation of 20% each. Calculation of packing attenuation was performed with the use of an on-line cerebral aneurysm calculator software (www.angiocalc.com) with a 2D spherical function with a diameter of 23 mm for aneurysm volume calculation. The silicon aneurysm models were connected for imaging to a pulsating circulatory pump (Medos VAD; Medos Medizintechnik AG, Stolberg, Germany) with a frequency of pulsation of 80 beats per minute, a flow volume of 300 mL/min, and a systolic speed of 80–100 cm/s.

Imaging Protocol

DSA was performed in a clinical angiography suite (Axiom Artis z; Siemens, Erlangen, Germany) with the use of 10-mL hand injections of iodinated contrast material (Iopamiro 300; Bracco, Milano, Italy).

On the table, noncontrast FP-CT (DynaCT, Siemens) was performed for the in vitro experiments with the use of the following parameters: 20-second acquisition, 0.4° increment, 512 × 512 matrix, 220° total angle, 20°/s, and 15 frames per second.

MRI was performed with the use of a 3T clinical MR scanner (Magnetom Trio, Siemens) with a 32-channel head coil (Siemens). Imaging was performed with a routine scanning protocol by use of a 3D TOF sequence (TR, 22; TE, 3.9; flip angle, 18; matrix, 384 × 224; FOV, 166 × 200; voxel size, 0.5 × 0.5 × 0.6 mm), T2 (TR, 5470 ms; TE, 81 ms; matrix, 512 × 314; FOV, 180 × 180 mm), T1 (TR, 250 ms; TE, 3 ms; matrix, 224 × 512; FOV, 180 × 180 mm), and, in addition, B0 (TR, 488 ms; TE, 5.2 ms; matrix, 64 × 64; FOV, 192 × 192 mm) and true fast imaging with steady state precession (TR, 4.4; TE, 2.2 ms; matrix, 256 × 256; FOV, 200 × 200) sequences in the in vitro experiments.

CT and CTA were performed by use of an 8-row multidetector clinical CT scanner (LightSpeed Ultra, GE Healthcare, Milwaukee, Wisconsin). CT was performed with the use of the following parameters: 140 kV; 70 mAs; section thickness, 1.25 mm; table increment, 2.01 mm; FOV, 250 × 250. CTA in the in vivo experiment was carried out by use of hand injection of 10 mL of iodinated contrast (Iopamiro 300) through the groin sheath left in place for imaging after the coiling procedure. CTA was triggered visually on a transverse section of the descending aorta at the level of the heart when contrast media opacification became visible.

Postprocessing was performed on a workstation for viewing and creation of multiplanar reformatted images (Syngo Workplace, Siemens).

Experimental Aneurysm Creation: Animal Model

All procedures were performed according to local regulations and were approved by the responsible local authorities. Experimental bifurcation aneurysms were surgically created in 4 female adult New Zealand White rabbits (3–4.5 kg). All animals were anesthetized with an intramuscular injection of ketamine (65 mg/kg) and xylazine (5 mg/kg) 30 minutes before surgery, which was repeated if necessary during the procedure. Carotid bifurcation aneurysms were surgically created as previously described,[20] by means of a modification of the venous pouch aneurysm model to create aneurysms >10 mm in diameter. In brief, a venous pouch was created from a 1- to 1.5-cm-long section of the jugular vein. The right common carotid artery was temporarily clipped, and an oval arteriotomy was performed. The left common carotid artery was temporarily clipped proximally and permanently ligated distally. The left common carotid artery was then cut proximally to the ligature. The proximal part of the left common carotid artery was mobilized to the right side to create an end-to-side anastomosis of the left-to-right common carotid artery to the proximal part of the arteriotomy by use of single-knot 10–0 nylon sutures. The venous pouch was finally sutured into the resulting arteriotomy defect in this artificial vessel bifurcation (Fig 6 *A*, *-B*). Four weeks after surgery, the aneurysms were embolized through a 5F sheath in the right femoral artery as completely as possible with poly-

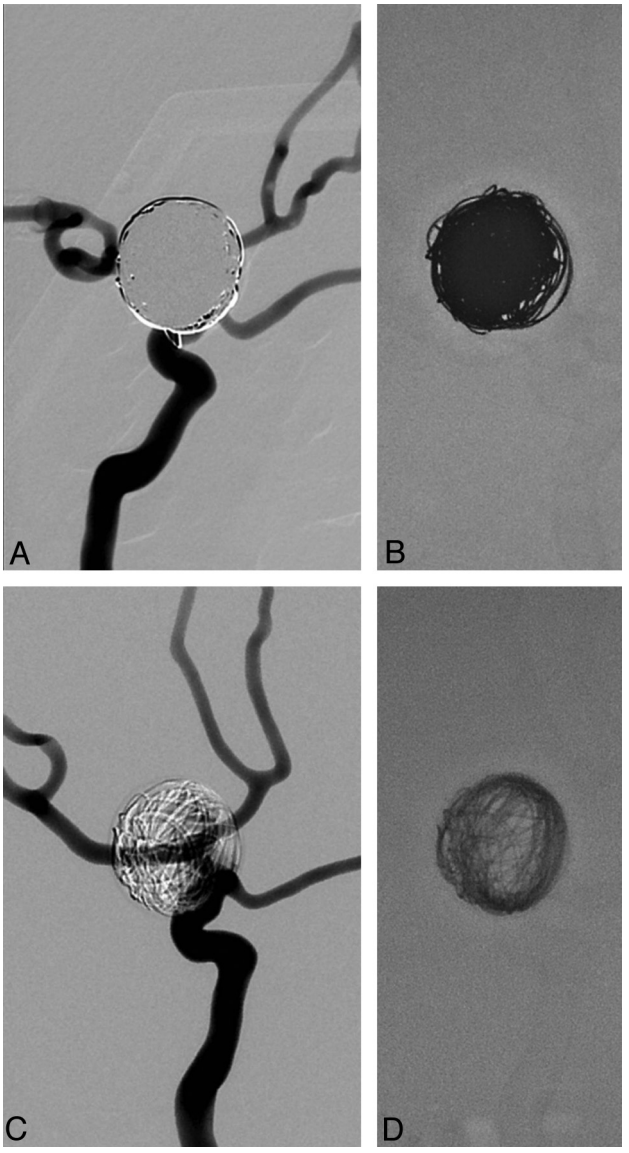

FIG 2. DSA of the in vitro silicon aneurysm model coiled with a calculated packing attenuation of 20%. Note the transparency of the polymeric coils *(C)* with persistent visualization of the superimposed vessel anatomy, which is completely obscured by standard platinum coils *(A)*. Fluoroscopic images show the difference in radio-opacity of polymeric *(D)* and standard platinum coils *(B)*.

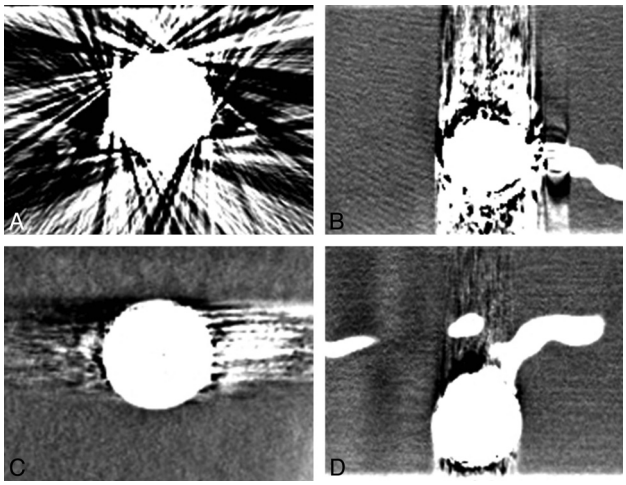

FIG 3. Flat panel CT images of standard platinum coils *(A* and *B)* and polymeric coils *(C* and *D)*. Note significant artifact reduction of polymeric coils compared with standard platinum coils; however, visualization of the peri-aneurysmal area is still significantly impaired.

meric coils. DSA, CT, CTA, and MR imaging were performed immediately after endovascular treatment. The animals were euthanized immediately after the experiment by a lethal injection of sodium pentobarbital (400 mg/kg intra-peritoneally).

Evaluation Criteria

The images from the in vitro DSA were qualitatively evaluated for transparency and visibility of superimposed vessels (visible, not visible). The FP-CT, CT/CTA, and MR images were evaluated for artifact production (none, minor, major), visibility of individual coils, coil mass, residual aneurysm, and peri-aneurysmal area for diagnostic value (not acceptable, acceptable, excellent). All scores were assessed in consensus by the authors (P.M. and J.G.).

RESULTS

Qualitative assessment scores for the in vitro and in vivo experiments are summarized in the On-line Table. Overall, in vitro and in vivo imaging demonstrated reduced artifact production and higher scoring assessments for polymeric coils in all imaging modalities compared with standard platinum coils.

On DSA, polymeric coils demonstrated transparency that permitted visualization of superimposed vessel structures in vitro and in vivo, whereas platinum coils were not transparent and completely masked superimposed vessel structures because of their high radio-attenuation (Figs 2 and 6). Polymeric coils showed satisfying radio-opacity and visibility under fluoroscopy for safe and controlled endovascular coil delivery. FP-CT in vitro demonstrated improved image quality as the result of reduced artifact production by use of polymeric coils compared with standard platinum coils. However, the image quality was still not of full diagnostic value for both coil materials because of massive beam-hardening and streak artifacts (Fig 3). Image quality of CT and MR imaging was improved by use of polymeric coils, which permitted enhanced depiction of individual coil loops and residual aneurysm lumen as well as the peri-aneurysmal area (Figs 4 and 5). Susceptibility artifacts in vitro on B0 images were not visible with the use of polymeric coils. TOF imaging demonstrated residual flow in the aneurysm sac and neck area in both coil groups; however, this was improved and rated excellent for polymeric coils (Fig 5). In vivo MRI in aneurysms embolized with polymeric coils was able to depict the aneurysm wall and the surrounding soft tissue without obscuring susceptibility artifacts by use of T1WI and even more accurately delineated on T2WI (Fig 6). Remarkably, CT images demonstrated considerably improved image quality with only minor artifact production compared with standard platinum coils. Depiction of the embolic mass, individual coils, and the peri-aneurysmal area on CT and residual intra-aneurysmal flow on CTA was considered acceptable for diagnostic purposes by use of polymeric coils. On the other hand, CT image quality with the use of standard platinum coils was not acceptable because of extensive beam-hardening and streak artifacts that obscured the area of interest (Figs 4, 6, and 7).

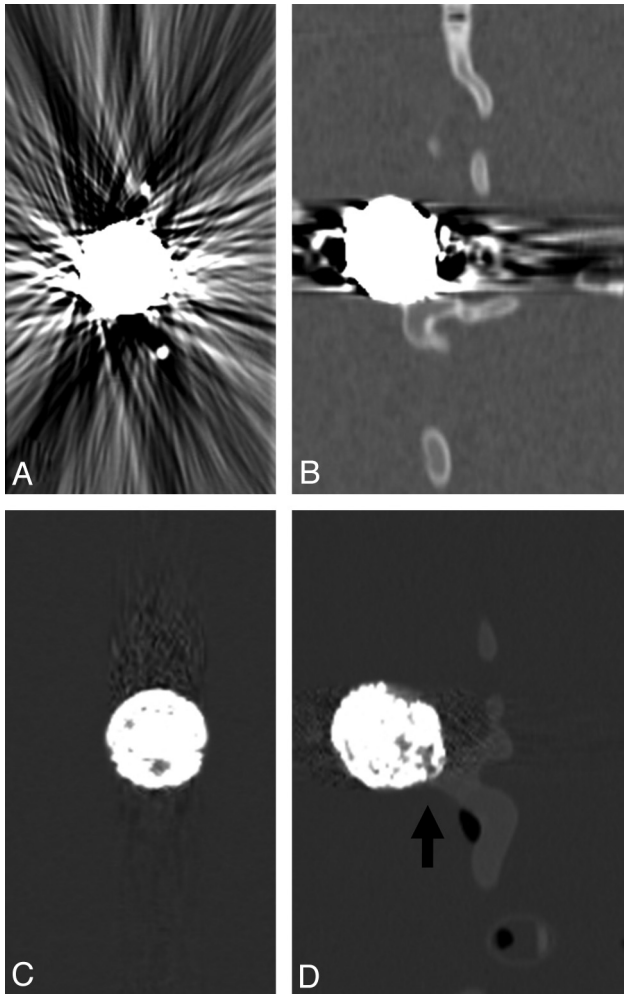

FIG 4. CT scan of standard platinum coils *(A* and *B)* and polymeric coils *(C* and *D)*. Note significant reduction of beam-hardening artifacts compared with standard platinum coils. In the aneurysm embolized with polymeric coils, individual coils as well as residual aneurysm lumen and neck (*arrow*) can be distinguished.

DISCUSSION

Endovascular coiling has become a well-established and increasingly performed treatment technique for ruptured and unruptured intracranial aneurysms.[1] However, because of the risk of aneurysm re-growth and neck recurrence after coil treatment,

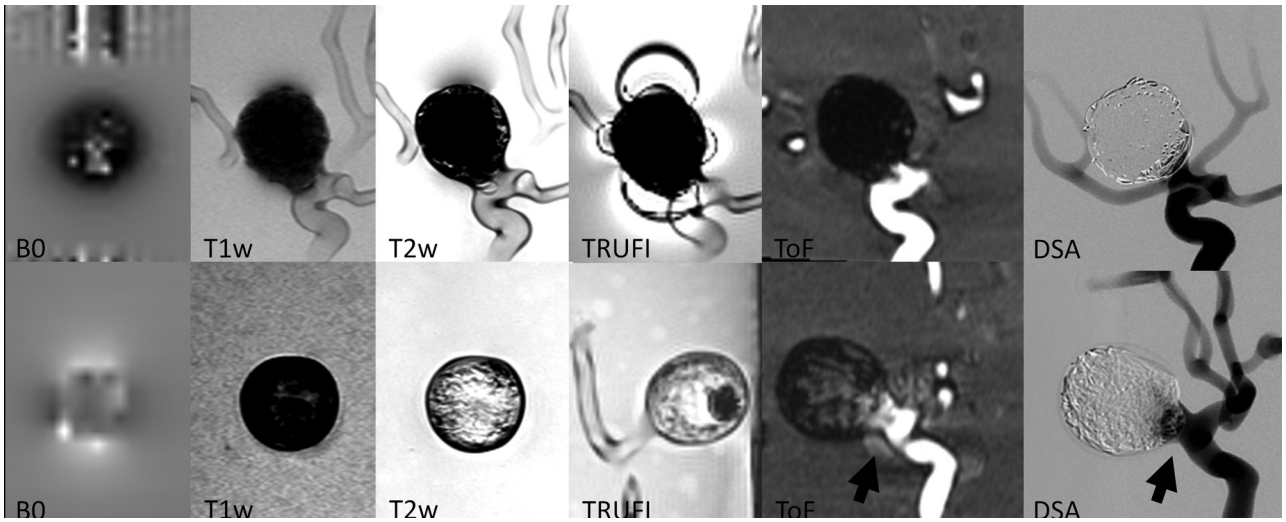

FIG 5. MR images and corresponding DSA of standard platinum coils (upper row) and polymeric coils (lower row) in vitro. Less magnetic field distortion and artifact production are seen with polymeric coils with the use of MRI. Individual coils can be distinguished in T2WI, TRUFI (true fast imaging with steady state precession), and TOF images as compared with standard coils. Note the visualization of residual flow within the aneurysm sac and the neck area in the aneurysm treated with polymeric coils in the TOF and DSA (*arrows*) compared with standard platinum coils at the same packing attenuation.

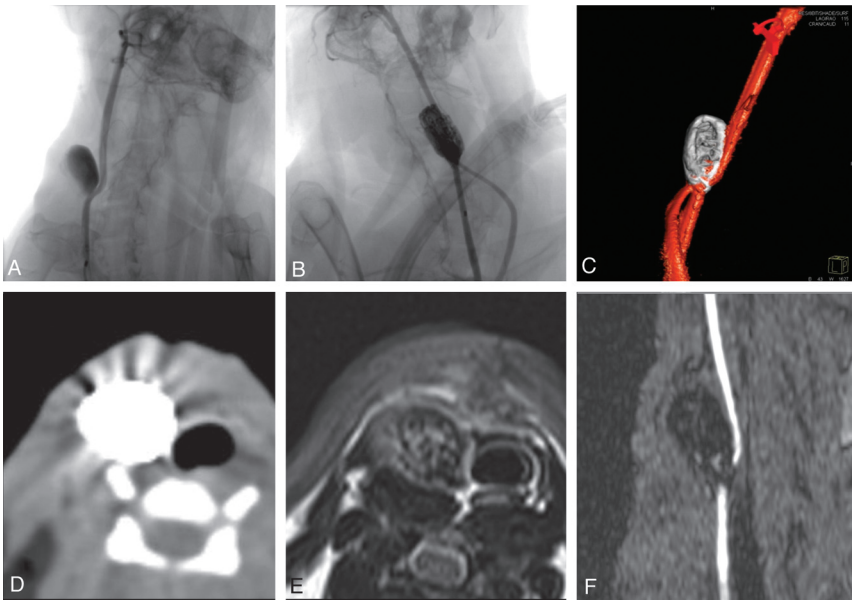

FIG 6. DSA demonstrates the anatomy of the venous patch carotid artery bifurcation model with the anastomosis of the left carotid artery proximal to the aneurysm *(A* and *B)*. Posttreatment DSA *(B)* and 3D rotational angiography *(C)* show complete obliteration of the aneurysm *(B)*. Note the persistent visibility of the right carotid artery despite superimposition by the coil mass. Note the minor effect of beam-hardening artifacts on the surrounding soft tissue on CT imaging *(D)*. MR images demonstrate visibility of individual coil loops in the T2WI *(E)* and the lack of intra-aneurysmal flow in the TOF image *(F)*.

follow-up imaging is mandatory. DSA has been used as the criterion standard for follow-up assessment of coiled aneurysms. However, diagnostic DSA is an invasive, comparatively expensive, and time-consuming procedure with the potential risk of clinical complications.[21,22] To overcome the disadvantages of DSA noninvasive imaging, follow-up is performed as an alternative. Imaging artifacts caused by the metallic nature of coils are an important factor influencing the quality of posttreatment imaging. MRI/MRA has been increasingly used as the imaging technique of choice for posttreatment follow-up of coiled aneurysms.[9,11,15,16,23-25] However, despite encouraging imaging quality and improving artifact reduction of MRI/MRA, disadvantages of this technique include comparatively long examination time, limited availability, and contraindication for patients with pacemakers and biostimulators. Metallic implants cause massive beam-hardening and streak artifacts on CT images, which deteriorate image quality and furthermore superimpose other brain structures of interest. The metallic nature of standard platinum coils precludes the use of CT or CTA as imaging techniques after coil treatment.[26,27] Therefore, from an imaging point of view, an optimal coil material would permit artifact-free imaging or cause the least possible imaging artifacts and would allow reliable and accurate imaging diagnosis. Polymeric-based coil material has the potential to offer these features. However, to date, only limited data about metal-free polymeric-based embolic material for the treatment of intracranial aneurysms are available. Hydrogel filaments opacified with barium sulfate or iodine have been used in experimental studies to evaluate occlusion of aneurysms on CT and CTA. These studies have shown promising results in detecting aneurysmal remnants after treatment with hydrogel filaments and demonstrate the potential of CTA to provide images suitable to determine whether re-treatment is necessary.[17-19]

The present study, through the use of different imaging modalities, has demonstrated that polymeric coils cause less imaging artifacts compared with standard platinum coils on all imaging modalities. Overall, they provided better imaging and visualiza-

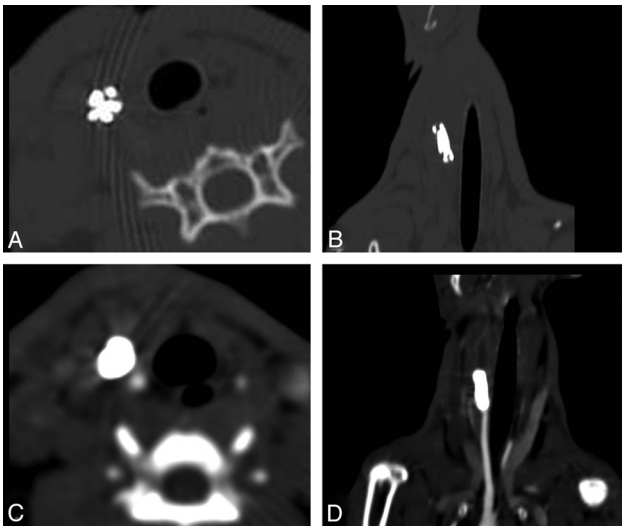

FIG 7. CT images of a coiled carotid bifurcation aneurysm. Note the reduced artifact production and visibility of individual coils on the unenhanced CT scan *(A* and *B)*. CTA shows complete occlusion of the aneurysm and minimal artifact production *(C* and *D)*.

tion of the coil mass, coil details, and the soft tissue area adjacent to the embolized aneurysm. Therefore, polymeric coils might be able to improve posttreatment surveillance as well as detection and avoidance of peri-procedural complications.

MRI examinations in vitro as well as in vivo have demonstrated excellent visualization of details of the coil mass and individual coils. With the use of TOF sequences, the presence of residual flow within an embolized aneurysm was visible, a feature of greatest significance for follow-up imaging of coiled aneurysms. The lack of susceptibility artifacts demonstrated on B0 images permits artifact-free imaging of soft tissue structures immediately adjacent to the embolized aneurysm on T1WI and T2WI. Furthermore, detailed depiction of the aneurysm wall could be achieved in the experimentally created in vivo aneurysms.

On conventional CT, the aneurysms embolized with polymeric coils demonstrated only minimal beam-hardening and streak artifacts. The beam-hardening artifacts of the polymeric coils were significantly reduced compared with platinum coils, with only minimal residual artifacts. The improved image quality allowed depiction of single-coil loops and residual aneurysm lumen. In our opinion, the residual artifacts are caused by the tantalum added to the polymer to gain some radio-opacity for visualization of the coil strand on fluoroscopy during the procedure. This artifact reduction may significantly improve diagnostic accuracy of posttreatment CT examinations. CT has an important role in the emergency and acute settings of subarachnoid hemorrhage to recognize potential hemorrhagic complications and rebleedings, which can be masked by metallic coil artifacts. Furthermore, position of single coils and coil loops could be visualized, a feature that is of accurate.

The endovascular treatment of large and giant aneurysms may still necessitate the introduction of considerably large coil masses. Superimposition of a radio-attenuated coil mass may impair visualization of vessel structures of interest, especially in the treatment of complex aneurysms and in aneurysms with vessels arising near or at the aneurysm neck. In some clinical settings, incomplete treatment caused by insufficient visualization of crucial anatomic information must be accepted to avoid inadvertent vessel occlusion. Furthermore, DSA has been shown to be less accurate in detecting aneurysm body remnants extending or invaginating into the coil mass. Coils surrounding the aneurysmal remnant form a radio-attenuated, helmet-like mass around the remnant, causing difficulties in delineating the remnant, a phenomenon previously referred to as the helmet effect.[16] The DSA examinations in the current study have demonstrated excellent visibility of superimposed vessel structures through the coil mass during and after coiling. This feature may improve procedural safety and efficacy of the treatment or re-treatment of complex and large to giant cerebral aneurysms.

On the other hand, reduced radio-opacity of the polymeric coil system might also cause potential disadvantages in the clinical setting. Visual assessment and determination of adequacy of coil packing and residual filling of a treated aneurysm might be more difficult to judge as compared with platinum coils because of the better appreciation of these findings. Furthermore, the polymeric coils are less fluoroscopically visible than platinum coils, and overlapping bone and soft tissue structures might further impede intraprocedural visibility. Last, because the system consists of a polymer strand without preformed loops, it must bend at the aneurysm wall to adapt to the aneurysm geometry, which makes the system more rigid to place within an aneurysm compared with similar-sized platinum coils.

Although the present experimental study has shown promising imaging characteristics of polymeric coils and potential implications for clinical management, it has its inherent limitations. First, only a small sample of in vitro and in vivo imaging was performed and qualitatively analyzed. The study was conducted with the aim to preliminarily evaluate the imaging characteristics and artifact production of a polymeric-based coil system through the use of different imaging modalities compared with standard platinum coils. Second, these preliminary imaging findings must be further investigated in experimental and clinical studies, which are lacking at the moment. Clinically significant properties such as potential thrombogenicity and biologic behavior of the coil mass as well as the durability of the treatment compared with standard coils have not been addressed in this study. Last, the clinical value of reduced imaging artifacts and especially the potential role of CT/CTA examinations in the acute setting and during follow-up of endovascular aneurysm treatment must be further established.

CONCLUSIONS

This initial experimental study demonstrated improved imaging quality with the use of polymeric coils compared with standard platinum coils in all examined imaging modalities. Artifact reduction permits better visualization of coils and coil loops as well as the surrounding soft tissue. This might be advantageous for improved intraprocedural imaging for the detection of complications and posttreatment noninvasive follow-up imaging. Further investigation and evaluation of the clinical value and imaging characteristics of polymeric embolization material is needed.

Disclosures: Pasquale Mordasini—*RELATED: Grant:* P.M. was supported by a scientific grant of the Swiss Foundation for Grants in Biology and Medicine (SFGBM). James Byrne—*UNRELATED: Board Membership:* Codman Neurovascular, Comments: SAB member; *Grants/Grants Pending:* Balt International,* Siemens AG*; *Royalties:* Springer-Verlag, Comments: Portion of book sales. Michael Reinert—*UNRELATED: Consultancy:* Oxygen Biotherapeutics.* Jan Gralla—*UNRELATED: Consultancy:* Covidien–Ischemic Stroke Intervention*; *Grants/Grants Pending:* Swiss National Foundation* (**money paid to institution*).

REFERENCES

1. Molyneux AJ, Kerr RS, Yu LM, et al. **International Subarachnoid Aneurysm Trial (ISAT) of neurosurgical clipping versus endovascular coiling in 2143 patients with ruptured intracranial aneurysms: a randomised comparison of effects on survival, dependency, seizures, rebleeding, subgroups, and aneurysm occlusion.** *Lancet* 2005;366:809–17
2. Byrne JV, Sohn MJ, Molyneux AJ, et al. **Five-year experience in using coil embolization for ruptured intracranial aneurysms: outcomes and incidence of late rebleeding.** *J Neurosurg* 1999;90:656–63
3. Raymond J, Guilbert F, Weill A, et al. **Long-term angiographic recurrences after selective endovascular treatment of aneurysms with detachable coils.** *Stroke* 2003;34:1398–403
4. Kang HS, Han MH, Kwon BJ, et al. **Repeat endovascular treatment in post-embolization recurrent intracranial aneurysms.** *Neurosurgery* 2006;58:60–70
5. Campi A, Ramzi N, Molyneux AJ, et al. **Retreatment of ruptured cerebral aneurysms in patients randomized by coiling or clipping in the International Subarachnoid Aneurysm Trial (ISAT).** *Stroke* 2007;38:1538–44
6. Fernandez ZA, Guglielmi G, Vinuela F, et al. **Endovascular occlusion of intracranial aneurysms with electrically detachable coils: correlation of aneurysm neck size and treatment results.** *AJNR Am J Neuroradiol* 1994;15:815–20
7. Ries T, Siemonsen S, Thomalla G, et al. **Long-term follow-up of cerebral aneurysms after endovascular therapy prediction and outcome of retreatment.** *AJNR Am J Neuroradiol* 2007;28:1755–61
8. Bakker NA, Westerlaan HE, Metzemaekers JD, et al. **Feasibility of magnetic resonance angiography (MRA) follow-up as the primary imaging modality after coiling of intracranial aneurysms.** *Acta Radiol* 2010;51:226–32
9. Ferre JC, Carsin-Nicol B, Morandi X, et al. **Time-of-flight MR angiography at 3T versus digital subtraction angiography in the imaging follow-up of 51 intracranial aneurysms treated with coils.** *Eur J Radiol* 2009;72:365–69
10. Wallace RC, Karis JP, Partovi S, et al. **Noninvasive imaging of treated cerebral aneurysms, part I: MR angiographic follow-up of coiled aneurysms.** *AJNR Am J Neuroradiol* 2007;28:1001–08
11. Urbach H, Dorenbeck U, von Falkenhausen M, et al. **Three-dimensional time-of-flight MR angiography at 3 T compared to digital subtraction angiography in the follow-up of ruptured and coiled intracranial aneurysms: a prospective study.** *Neuroradiology* 2008;50:383–89
12. Gonner F, Heid O, Remonda L, et al. **MR angiography with ultrashort echo time in cerebral aneurysms treated with Guglielmi detachable coils.** *AJNR Am J Neuroradiol* 1998;19:1324–28
13. Walker MT, Tsai J, Parish T, et al. **MR angiographic evaluation of platinum coil packs at 1.5T and 3T: an in vitro assessment of artifact production: technical note.** *AJNR Am J Neuroradiol* 2005;26:848–53
14. Hennemeyer CT, Wicklow K, Feinberg DA, et al. **In vitro evaluation of platinum Guglielmi detachable coils at 3 T with a porcine model: safety issues and artifacts.** *Radiology* 2001;219:732–37
15. Gauvrit JY, Leclerc X, Caron S, et al. **Intracranial aneurysms treated with Guglielmi detachable coils: imaging follow-up with contrast-enhanced MR angiography.** *Stroke* 2006;37:1033–37
16. Agid R, Willinsky RA, Lee SK, et al. **Characterization of aneurysm remnants after endovascular treatment: contrast-enhanced MR angiography versus catheter digital subtraction angiography.** *AJNR Am J Neuroradiol* 2008;29:1570–74
17. Constant MJ, Keeley EM, Cruise GM. **Preparation, characterization, and evaluation of radiopaque hydrogel filaments for endovascular embolization.** *J Biomed Mater Res B Appl Biomater* 2009;89:306–13
18. McCoy MR, Cruise GM, Killer M. **Angiographic and artefact-free computed tomography imaging of experimental aneurysms embolised with hydrogel filaments.** *Eur Radiol* 2010;20:870–76
19. Killer M, McCoy MR, Vestal MC, et al. **Use of CT angiography in comparison with other imaging techniques for the determination of embolus and remnant size in experimental aneurysms embolized with hydrogel filaments.** *AJNR Am J Neuroradiol* 2011;32:923–28
20. Forrest MD, O'Reilly GV. **Production of experimental aneurysms at a surgically created arterial bifurcation.** *AJNR Am J Neuroradiol* 1989;10:400–02
21. Willinsky RA, Taylor SM, TerBrugge K, et al. **Neurologic complications of cerebral angiography: prospective analysis of 2,899 procedures and review of the literature.** *Radiology* 2003;227:522–28
22. Kaufmann TJ, Huston J III, Mandrekar JN, et al. **Complications of diagnostic cerebral angiography: evaluation of 19,826 consecutive patients.** *Radiology* 2007;243:812–19
23. Anzalone N, Scomazzoni F, Cirillo M, et al. **Follow-up of coiled cerebral aneurysms: comparison of three-dimensional time-of-flight magnetic resonance angiography at 3 Tesla with three-dimensional time-of-flight magnetic resonance angiography and contrast-enhanced magnetic resonance angiography at 1.5 Tesla.** *Invest Radiol* 2008;43:559–67
24. Sprengers ME, Schaafsma JD, van Rooij WJ, et al. **Evaluation of the occlusion status of coiled intracranial aneurysms with MR angiography at 3T: is contrast enhancement necessary?** *AJNR Am J Neuroradiol* 2009;30:1665–71
25. Pierot L, Portefaix C, Boulin A, et al. **Follow-up of coiled intracranial aneurysms: comparison of 3D time-of-flight and contrast-enhanced magnetic resonance angiography at 3T in a large, prospective series.** *Eur Radiol* 2012;22:2255–63
26. Richter G, Engelhorn T, Struffert T, et al. **Flat panel detector angiographic CT for stent-assisted coil embolization of broad-based cerebral aneurysms.** *AJNR Am J Neuroradiol* 2007;28:1902–08
27. Masaryk AM, Frayne R, Unal O, et al. **Utility of CT angiography and MR angiography for the follow-up of experimental aneurysms treated with stents or Guglielmi detachable coils.** *AJNR Am J Neuroradiol* 2000;21:1523–31